

Lasers in Eng., Vol. 46, pp. 313–320
Reprints available directly from the publisher
Photocopying permitted by license only

©2020 Old City Publishing, Inc.
Published by license under the OCP Science imprint,
a member of the Old City Publishing Group

Porosity Control of *In Situ* Forming Tungsten Carbide in Laser Additive Manufacturing (LAM)

P. SEVCENKO^{1,*}, A. CHRYSANTHOU¹, C.Y. KONG² AND P. NICOLSON²

¹*University of Hertfordshire, Hatfield, Hertfordshire, AL10 9AB, UK*

²*C4 Carbides Ltd., 9 Nuffield Rd, Cambridge, CB4 1TF, UK*

The effect of powder compression on the formation of porosity when heating with a laser beam has been investigated. The starting materials were elemental powders of Fe, W and C which were locally melted to form WC in Fe matrix by an *in situ* laser additive manufacturing (LAM) process. The resulting microstructures have been studied and chemical analysis has been performed. The main application for the process is for the production of WC based or carbide cutting tooling by very accurate deposition of hard-facing materials onto a steel substrate. Fe is used as the matrix material since ferrous alloys are employed as the substrate for these applications.

Keywords: Fibre laser, tungsten carbide, WC, laser additive manufacturing (LAM), in situ tungsten carbide formation, porosity control

1 INTRODUCTION

Laser additive manufacturing (LAM) can be used to produce hard-facing and abrasive materials by re-melting of the matrix metals present in specifically sintered powders which contain already formed ceramic particles; for example, WC in a Co matrix. Such sintered powders are widely available off the shelf; however, the process limits the hardness of the deposit, lacks control over the forming microstructure and has a very narrow processing window,

*Corresponding author: E-mail: p.sevcenko2@herts.ac.uk

often with low processing speed. These limitations have hindered the wider adoption of AM in hard-facing applications.

An approach using the *in situ* formation of carbide particles from elemental powders with increased hardness has been reported [1, 2]. In addition, greater control over the resulting microstructure can be achieved by modifying the powder composition. The *in situ* formation process, however, is not well represented in the additive manufacturing (AM) industry. The application of AM to produce cutting tools is further restricted as more traditional methods are used. High pressure sintering is the main process to produce carbide tooling at the moment. The process is very energy and time consuming as it involves pressing, moulding into final shape, dewaxing, pre-sintering, sintering, post-sintering and finishing operations [3]. The resulting material often requires further mounting to the tool substrate and grinding. The resulting tool is of very high hardness up to 2250 HV and toughness up to 30 MPa/m².

A recent study, however, by C4 Carbides, Ltd. has shown that approximately 1% of the entire hard-metal material is used for cutting. The rest is ground away or discarded after the tool is damaged or dulled. This, coupled with the fact that Co and W are on the list of critical raw materials for the EU, as published by the European Commission [4], makes the precise deposition of these materials an attractive alternative to conventional methods.

The application of AM processes to produce hard-metal deposits using a pre-blended mixture of Co binder, Cr and the WC carbide has been patented [5]. This report presents preliminary studies of an *in situ* formation of WC in Fe matrix. In particular, the effect of the powder pressing prior to heating is investigated using elementary powders of Fe, W and C to form a WC 12 wt.% Fe hard metals.

2 EXPERIMENTAL PROCEDURES

The starting materials of Fe 99.9% purity, <10 µm particle size (Alfa Aesar, GmbH); W, 99.9% purity, <25 µm particle size (Goodfellow, Ltd.) and C 99.9 purity synthetic, <20 µm particle size (Sigma-Aldrich Corporation) in elemental powder form were weighed out in 12Fe:82.6W:5.4C wt.% ratios to match the WC 12 wt.% Fe composition. The materials were then mixed in a planetary mill (PULVERISETTE 6; FRITSCH) without grinding media for 1 hour at 100 rpm with changing rotation direction every 20 seconds. From the same batch, two 0.5 g samples were prepared. Sample A was left in loose powder form and Sample B was pressed into an 8 mm diameter pellet under 100 MPa in a steel die. Both samples were placed in alumina crucibles. The top surface of Sample A was levelled with a spatula without applying pressure to provide a flat surface to focus the laser beam.

A 1 kW continuous wave (CW) fibre laser (redPOWER QUBE 1 kW; SPI Lasers, Ltd.) with a 5 mm diameter Gaussian beam emitted at 1025 nm was focused on the top surface of each sample in order to supply the heat. The laser was fired at 600 W requested power in the same focus spot of each sample for 3 seconds without scanning.

The products were cleared from any unreacted powders and prepared for microstructure analysis. The microstructures have been analysed using a scanning electron microscope (SEM) (JSM-5600; JEOL, Ltd.) combined with energy dispersive X-ray (EDAX) analysis (Genesis Spectrum v5.2) for chemical composition analysis. The grain size and porosity levels were measured using open source ImageJ [6] image processing software.

3 RESULTS

3.1 Porosity

As Figure 1 shows, Sample A solidified into a 0.097 g sphere of about 3mm diameter which has formed on the area of the laser beam focus. The remaining powder stayed in powder form and did not react accounting for 80.6% of the entire Sample A weight. Sample B retained the shape of a pellet - approximately 2.7 mm high and 7.8 mm diameter (see Figure 1) with a void formed at the laser beam focus area resulting in a 0.340 g sample and there was no free, unreacted powder left in the crucible.

From Figure 2 the microstructure of Sample A showed relatively low porosity of 4% with few large pores of 50 to 100 μm in diameter. The porosity of Sample B was relatively high at 16% and evenly dispersed across the entire sample with average pore size of 20 to 25 μm in diameter. Closer to the laser beam focus area the pores have agglomerated into larger pores approximately 500 μm in diameter.

3.2 Microstructure

3.2.1 General findings

The M_6C and WC carbides are expected to precipitate from the formed Fe-W melt pool and form by heterogeneous nucleation [2, 3, 7]. Agglomeration of



FIGURE 1

Photograph showing (left-hand side) Sample A (loose powder) and (right-hand side) Sample B (compressed powder) reacted materials,

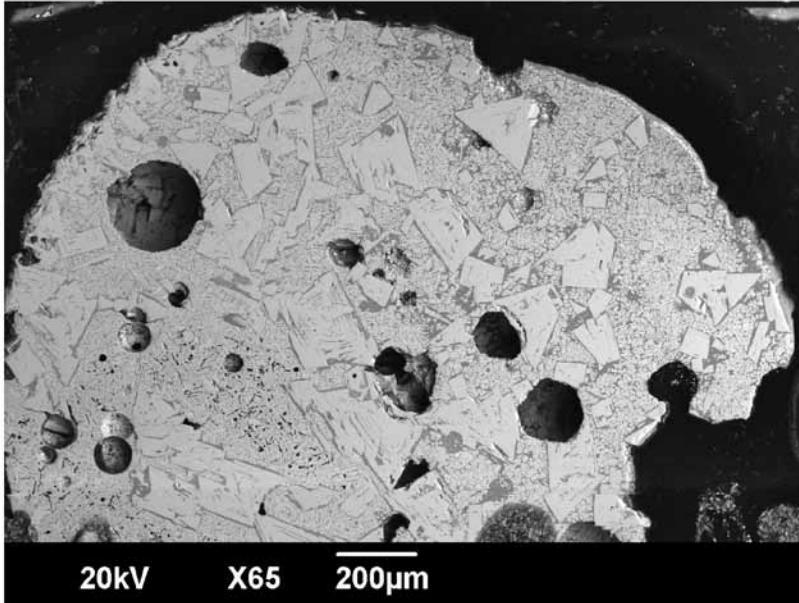


FIGURE 2
SEM micrograph showing Sample A microstructure with a 4% porosity.

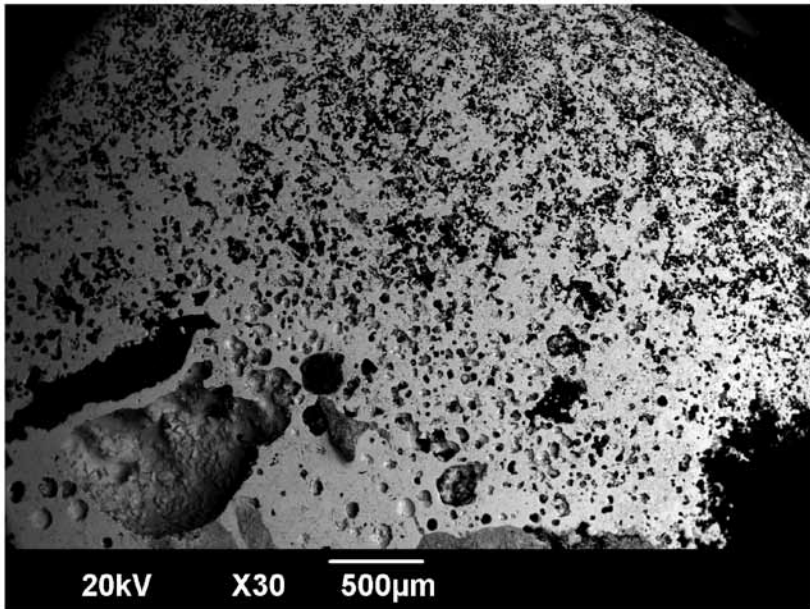


FIGURE 3
SEM micrograph showing Sample B microstructure with 16% porosity.

carbides is expected to take place with higher fraction of agglomerates closer to the laser beam focus area due to prolonged high temperatures and reduced heating rate compared to areas furthest from the heat source. In general, Sample B is expected to have more refined structure with less agglomeration of primary carbides due to lower maximum temperatures and greater surface area when compared to Sample A.

3.2.2 Observations for Sample A

The analysis of microstructure given in Figure 4 shows formation of primary and secondary mixed carbides with no free W, Fe or C present in the materials. The white colour particles which form in truncated triangle and triangular shapes that can be seen in Figure 4 contain approximately 36 at.% W, 63.5 at.% C and 0.9 at.% Fe. The content of C is highly exaggerated by the measuring equipment due to very low atomic weight of C and in comparison, very high atomic weight of W. Comparing the at.% of W and Fe suggests that the formed material is WC along with the less stable W_2C . Spherical white particles can also be observed in Figure 4 and show approximately 46 at.% W, 4.7 at.% Fe and 49.5 at.% C, the composition of these materials does not match the M_6C type carbides as they contain very low amounts of Fe and are likely also WC or W_2C carbides. Light grey particles form dendrites with 12.3 at.% W, 46.9 at.% Fe and 40.8 at.% C chemical composition which closely correspond with the chemical composition of Fe_3WC carbides. The average WC truncated triangle and triangular particles size is in range of 50 to 100 μm while the spherical particles are 6 to 10 μm with agglomerates reaching 30 μm in length.

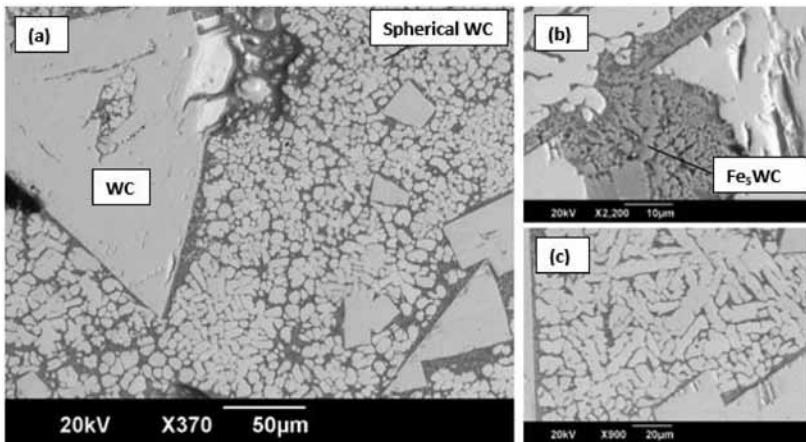


FIGURE 4

SEM micrographs showing Sample A microstructure: (a) WC (white particles); (b) Fe_3WC (grey particles); and (c) spherical WC (white particles) agglomeration.

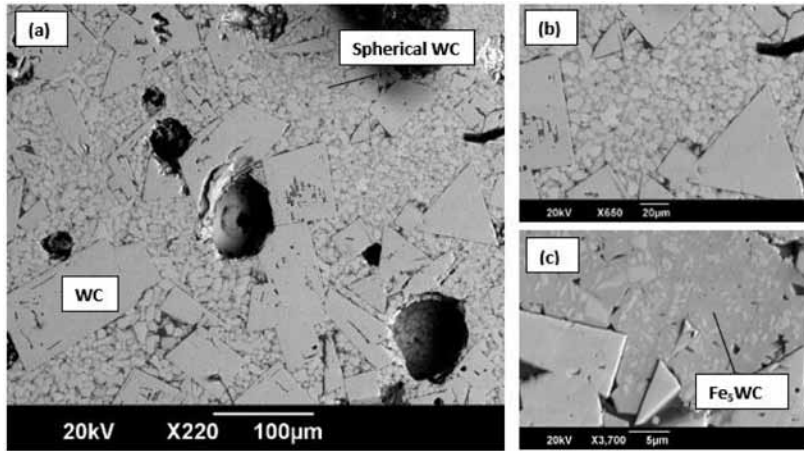


FIGURE 5

SEM micrographs showing Sample B microstructure: (a) WC (white particles); (b) Fe_5WC (grey particles) form around white WC spherical particle; and (c) Fe_5WC forms continuous matrix around white WC particles.

3.2.3 Observations for Sample B

Similar to Sample A, Sample B showed formation of carbides with no free W, Fe or C, as can be seen from Figure 5. White truncated triangle particles in Figure 5 contain approximately 37 at.% W, 62.7 at.% C and 0.8 at.% Fe, triangular particles 34 at.% W, 65 at.% C and 1.2 at.% Fe and spherical particles 35 at.% W, 65.2 at.% C, 1.1 at.% Fe. These compositions have been identified as WC and W_2C carbides. In Sample B, secondary carbides show chemical composition of 34.5 at.% W, 65 at.% C and 0.9 at.% Fe relating to Fe_5WC carbides. These carbides have formed around spherical WC carbides and have agglomerated to form a continuous matrix. The average WC truncated triangle and triangular particles size is in range of 10 to 100 μm . Spherical WC particles are between 6 to 15 μm in diameter. Secondary carbides of Fe_5WC show coring around the spherical WC particles and have agglomerated to form a continuous matrix.

4 DISCUSSION

The packing factor of the powders had significant impact on the resulting microstructures and porosities of materials. Contrary to expectations, the compressed sample has formed a more porous microstructure than the loose powder sample, 16% *versus* 4%, respectively. Closely packed powder particles formed evenly distributed pores and an increased heat affected zone (HAZ) around the laser beam focus area which has allowed the entire powder

to react and form a solid. Loose powders produced large, localized and agglomerated pores with a reduced HAZ.

The *in situ* formation of WC from elemental powders has been successfully achieved. WC has formed in a truncated triangle, triangular and spherical shapes. The formation of secondary carbides with M_6C structures (Fe_5WC) has taken place in both samples. These carbides have been formed in dendritic form in the loose powder sample and formed around spherical particles in the compressed powder sample agglomerating into a continuous matrix between the WC particles.

The closely packed particles in the compressed sample offered better heat distribution across the bulk of powder and allowed the heat to transfer across the entire sample. As a result, lower temperatures were reached across the entire compressed sample allowing the powder to sinter and retain the sample shape and powder particle positions. The loose powder sample was formed at a higher temperature and higher energy density melt pool under the laser beam, which, in the liquid phase has consumed the surrounding powder, but has left the powder away from the melt pool unreacted. The higher temperature reached in the loose powder sample has also promoted grain growth of WC.

5 CONCLUSIONS

This study has investigated the effect of compressing of the powders prior to heat treatment on the porosity and microstructure of *in situ* formation of WC 12 wt.% Fe hard-facing materials forming from elemental powders using a fibre laser beam as a heat source. The following conclusions have been drawn:

- (i) The compressed samples show increased porosity when compared to loose, untapped powders, 16% versus 4%, respectively;
- (ii) In both samples WC, Fe_5WC and possibly W_2C is forming. WC is forming in truncated triangle, triangular and spherical shapes. Fe_5WC is forming in the form of dendrites in the loose powders and around the spherical particles of WC in the compressed powders. The Fe_5WC within the compressed powders tended to agglomerate and form a continuous matrix between WC particles; and
- (iii) The compressed samples show an increased heat affected zone (HAZ) compared to the loose powders.

REFERENCES

- [1] Gu D-D. and Meiners W. Microstructure characteristics and formation mechanisms of *in situ* WC cemented carbide based hardmetals prepared by selective laser melting. *Materials Science & Engineering A. Structural Materials: Properties, Microstructure and Processing* 527(29-30) (2010), 7585-7592

- [2] Shu D., Li Z., Zhang K., Yao C., Li D. and Dai Z. *In situ* synthesized high volume fraction WC reinforced Ni-based coating by laser cladding. *Materials Letters* **195** (2017), 178-181
- [3] García J., Ciprés V.C., Blomqvist A. and Kaplan B. Cemented carbides microstructures: A review. *International Journal of Refractory Metals & Hard Materials* **80** (2019), 40-68
- [4] Deloitte Sustainability, British Geological Survey, Bureau de Recherches Geologiques et Minières, Netherlands Organisation for Applied Scientific Research (2017) *Report on Critical Materials for the EU, Critical Raw Materials profiles*. Brussels: Directorate-General for International Market, Industry, Entrepreneurship and SMEs.
- [5] Culf P.G. *Utility Knife Blade*. US Patent US 8,769,833 B2, 8th July 2014.
- [6] ImageJ, U.S. National Institutes of Health, Bethesda, Maryland, USA (1997-2018). Retrieved 8th January 2019 from, <https://imagej.nih.gov/ij/>.
- [7] Riabkina-Fishman M., Rabkin E., Levin P., Frage N., Dariel M.P., Weisheit A., Galun R. and Mordike B.L. Laser produced functionally graded tungsten carbide coatings on M2 high-speed tool steel. *Materials Science & Engineering A. Structural Materials: Properties, Microstructure and Processing* **302**(1) (2001), 106-114.